

Development and preliminary testing of an instrumented object for force analysis during grasping

R.A. Romeo¹, F. Cordella¹, L. Zollo¹, D. Formica¹, P. Saccomandi², E. Schena², G. Carpino¹,
A. Davalli³, R. Sacchetti³, and E. Guglielmelli¹

Abstract— This paper presents the design and realization of an instrumented object for force analysis during grasping. The object, with spherical shape, has been constructed with three contact areas in order to allow performing a tripod grasp. Force Sensing Resistor (FSR) sensors have been employed for normal force measurements, while an accelerometer has been used for slip detection. An electronic board for data acquisition has been embedded into the object, so that only the cables for power supply exit from it. Validation tests have been carried out for: (i) comparing the force measurements with a ground truth; (ii) assessing the capability of the accelerometer to detect slippage for different roughness values; (iii) evaluating object performance in grasp trials performed by a human subject.

I. INTRODUCTION

Force analysis during grasping is a fundamental issue to face while studying human grasping strategies as well as robotic grasping capabilities. Slippage detection is also essential to guarantee a stable grasp. Different approaches have been proposed in the literature to acquire information about the forces involved in the grasping action [1]. It is possible to distinguish between wearable and not-wearable solutions, respectively. Sensors embedded in gloves [2] or directly positioned on the hand [3] belong to the former one. A variety of instrumented objects, i.e. objects commonly grasped in everyday life embedding tactile or force sensors, belong to the latter one and have been adopted for studying grip force during pinch, tripod and power grasps. Different transduction technologies have been used in previous studies: force transducers [4,5], strain gauges [6,7], load cells [8], tactile sensors [9,10] for providing information about force values and spatial distribution of contact points, and six-axis force-torque sensors for determining the correct positioning of the fingers during tripod grasps [11], or for measuring the three components of the force applied during tripod grasp by human subjects [12,13] or else for multi-touch detection as in [14]. The main limitation of the object developed in [14] is

that it does not allow recognizing the forces applied by each finger during the contact. Furthermore, using six-axis F/T sensors implies very high costs.

The purpose of this work is to develop and test an instrumented object for grasp analysis that is: (i) able to individually analyze the force applied by each finger; (ii) capable of detecting slippage; (iii) based on low-cost technology easily applied to other types of objects for different grasps. The object is endowed with monoaxial force sensors for measuring the normal component of the applied force, and with an accelerometer for slippage detection during grasping. Force sensors embedded in the object have been statically calibrated and validated through a compared analysis with a sensorized robotic hand.

The use of accelerometers for slip detection dates back to the end of 80s. In [15,16], a slip sensor has been obtained placing an accelerometer on a rubber skin, which covered a plastic foam layer. Later, an additional accelerometer has been mounted in the sensor structure [17] to discriminate between vibration caused by the sensor itself and actual slippage. In [18], an accelerometer has been jointly used with a piezoelectric sensor. Slippage is recognized when both sensors overcome a certain threshold. In [19] an accelerometer has been used to verify the reliability of a pressure sensor to estimate slippage. However, the cited works do not report a systematic analysis of the use of the accelerometer to detect slippage. Furthermore, to the best of our knowledge, there are not previous examples of instrumented objects embedding accelerometers for slip analysis. In this work an ad hoc experimental setup for slip analysis has been developed: spectral analysis of accelerometer outputs has been performed to evaluate the sensor behavior when the object is slid thanks to a linear actuator upon surfaces with different *a priori* known roughness values. Afterwards, the instrumented object has been preliminary tested during tripod grasping tasks performed by one human subject.

II. INSTRUMENTED OBJECT

In order to study prehension forces in humans, tripod grasp has been initially selected, being one of the more commonly used Activities of Daily Living (ADLs, [20]). The object is a sphere with a diameter of 0.059 m, similar to a tennis ball. The location of the three contact areas (0.018x0.022 m) has been chosen according to [4]. The force sensors mounted on the contact areas boasted a continuous force resolution and a measurement range of [0.2, 20] N.

A. Design of the object

Figure 1b shows the CAD of the instrumented object. Inside, a cavity of 0.045 m diameter hosts the electronic

*This work was supported partly by the Italian Ministry of Instruction, University and Research with PRIN HandBot project (CUP: B81J12002680008) partly by the Italian Ministry of Health with NEMESIS Project (CUP: C81J12000380001), partly by the Neurohand project (DTB2 Filas) and partly by the INAIL with the PPR2 project (CUP: E58C13000990001).

¹R.A. Romeo, F. Cordella, L. Zollo, D. Formica, G. Carpino and E. Guglielmelli are with Laboratory of Biomedical Robotics and Biomicrosystems, Università Campus Bio-Medico di Roma, Roma, Italy {r.romeo, f.cordella, l.zollo, d.formica, g.carpino, e.guglielmelli}@unicampus.it.

²P. Saccomandi and E. Schena are with Unit of Measurements and Biomedical Instrumentation, Università Campus Bio-Medico di Roma, Roma, Italy {p.saccomandi, e.schena}@unicampus.it.

³A. Davalli and R. Sacchetti are with Centro Protesi INAIL, Budrio, Italy {a.davalli, r.sacchetti}@inail.it.

board. *Ad hoc* extrusions have been cut in the object inner walls to stick the board. The sensors have been directly connected to the board through *ad hoc* holes created within the object. A 0.013 m diameter hole has been designed to connect the board to an external DC power supply. The total weight of the instrumented object was around 0.06 kg.

Each contact area is composed of a quadrangular hole, with the sensor put in the middle, and a movable part with a cylindrical probe which allows conveying the applied normal force onto the sensitive part of the sensor. Very small mechanical springs (mean coil diameter: 0.001 m) have been mounted in five rails dug at the sides of the hole, in order to restore the equilibrium position of the movable parts. Although the chosen stiffness of the springs (0.004 N/m) avoids phenomena of pre-loading, it is worth noticing that a small amount of force is wasted onto the spring, i.e. 0.2 N per $50 \cdot 10^{-6}$ m of compression. This phenomenon is accounted for in the static calibration (see Section II.C).

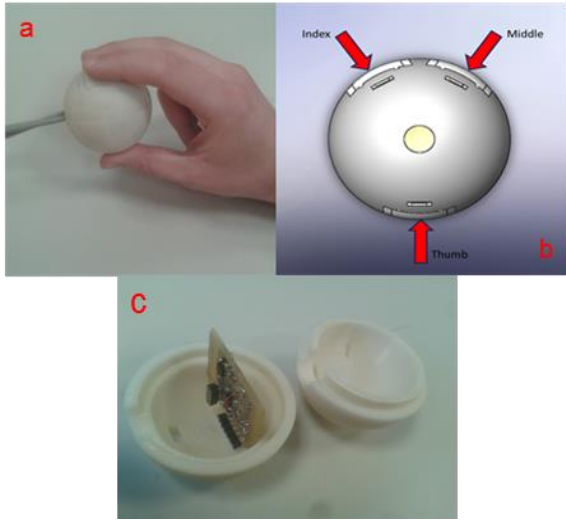


Fig. 1. Object grasped by human hand (a); CAD of the instrumented object (b). Detail of the etched board stuck in the object (c).

B. Tactile sensing: sensing element and electrical design

Forces applied to the object contact areas have been measured by Force Sensing Resistor sensors (FSR, Model 400 by Interlink Electronics, Inc.) mounted on the quadrangular hole of the object. Each sensor has a circular active area (diameter of 0.005 m), a discrimination threshold of 0.2 N and a measurement range up to 20 N. Its working principle is based on the transduction of the variation of an electrical resistance (R_{FSR}) into a force F : the higher is the force the lower is the resistance. Resistance value R_{FSR} has been transduced into voltage through a Wheatstone bridge with three nominally identical resistances $R_w = 2.2k\Omega$. An operational amplifier (TL074, Texas Instrument, Inc.) in differential configuration with a nominal gain of 2 amplified the bridge output. The voltage output can be expressed as:

$$V_{out} = \frac{c}{(R_w + 10^{\log_{10}(F)+b})} - d \quad (1)$$

where a and b are constants that depend on the sensor response, while c and d are constants that depend on the

actual gain of the amplification stage. The electronic board also includes a triaxial accelerometer (ADXL330 Analog Devices, Inc.) for slip detection and a dedicated voltage regulator (MCP1700, Microchip Technology, Inc.). The designed PCB (printed circuit board) has been fabricated through chemical etching and wedged in the object (Fig. 1C).

C. Static Calibration

The three FSR sensors (for thumb, index and middle fingers) have been statically characterized in order to extract the logarithmic relation between voltage and force. The best fitting calibration curves in the range 0.2-0.8 N, according to model in (1), are shown in Fig. 2. Experimental data have shown a good agreement with the non-linear theoretical model in (1) as confirmed by the high R^2 and the low RMSE (Table I). The mean sensitivity S_{mean} in the whole range of calibration has been $-0.37 \text{ V} \cdot \text{N}^{-1}$, $-0.32 \text{ V} \cdot \text{N}^{-1}$ and $-0.40 \text{ V} \cdot \text{N}^{-1}$ for thumb, index and medium, respectively.

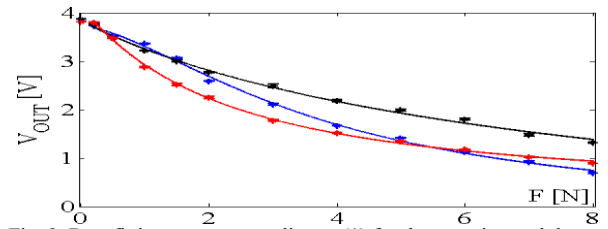


Fig. 2. Best fitting curves according to (1) for the experimental data (asterisks) obtained from FSRs static calibration.

TABLE I. RESULTS FROM FSRs CHARACTERIZATION.

Sensor	a	b	c	d	R^2	RMSE [V]	$S_{mean} [\text{V} \cdot \text{N}^{-1}]$	Discrimination threshold [N]
thumb	-1.58	4.26	-8542	-3.72	0.997	0.064	-0.37	0.2 N
index	-0.96	4.21	-10760	-3.83	0.996	0.064	-0.32	0.2 N
middle	-1.09	3.72	-8591	-4.07	0.999	0.038	-0.40	0.5 N

Moreover, hysteresis has also been analyzed. Three repeated cycles of load and unload have been carried out for each sensor; hysteresis has been calculated considering the maximum difference of V_{out} at the same F value, as a percentage of full-scale output range [21]. Hysteresis values (Fig.3) ranged from a minimum of 2.3% (for index sensor) to a maximum of 11.5% (for middle sensor), confirming the manufacturer specifications [22].

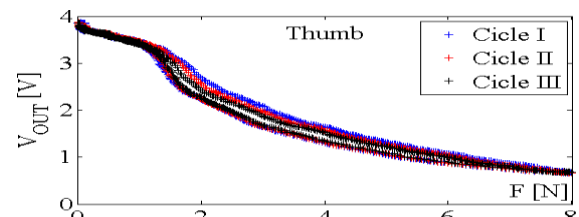


Fig. 3. Sequential tests for assessment of the hysteresis error (thumb).

III. EXPERIMENTAL TESTS AND RESULTS

In this section, experiments with relevant set-up will be illustrated. Three experimental sessions have been executed, with the following order: (i) validation of FSRs force measurements by means of a sensorized robotic hand; (ii) investigation on the object capability to detect slippage; (iii)

grasp analysis with a human subject. In every described trial, sensor outputs have been acquired by means of a DAQ board (NI-6009) at a sampling rate of 2000 Hz.

A. Comparison with a ground truth

In order to demonstrate the reliability of the force data acquired by the sensors embedded in the instrumented object, a compared analysis with the force values measured by a robotic hand (i.e., the DLR/HIT Hand II [23]) has been performed. Each finger of the robotic hand has three torque sensors and three Hall-effect sensors for measuring joint positions. By means of the hand Jacobian and the measured torques, the forces applied by the hand tips have been computed as follows:

$$F_{TIP}^{tip} = R_{mcp}^{tip} J_P^{-1} \tau^T = R_{mcp}^{tip} F_{TIP}^{MCP} \quad (2)$$

where R_{mcp}^{tip} is the rotation matrix of the MCP joint reference frame with respect to the fingertip reference frame, J_P^{-1} is the Jacobian matrix related to linear velocity, F_{TIP}^{MCP} is the force applied by the fingertip with respect to the MCP joint reference frame and F_{TIP}^{tip} is the fingertip force expressed in the fingertip reference frame.



Fig. 4. Robotic hand applying force on one sensorized area of the object.

The instrumented object has been located on a support (Fig. 4) and the normal force applied by the middle finger of the robotic hand on one sensorized area of the object surface has been simultaneously measured by the FSR sensor in the object and the torque sensors in the hand. Eight repetitions of the task have been performed.

Force mean value extracted from the torque sensors was equal to 3.3584N (± 0.1404), whereas, the corresponding force mean value recorded by FSRs was 3.3495N (± 0.1523). Therefore, it is possible to conclude that the forces acquired with the instrumented object are quite comparable to those measured from the torque sensors embedded in the robotic hand.

B. Slip detection

A specific experimental setup (Fig. 5a) was arranged to rigorously analyze slippage detection by means of the accelerometer embedded in the object. It consisted of a linear actuator, which translated the object onto three metallic surfaces with given roughness, i.e. $2 \cdot 10^{-7}$ m, $8 \cdot 10^{-7}$ m and $32 \cdot 10^{-7}$ m. The actuator (M-235.2DD by PI, Inc.) was position controlled by means of a PID servo control and an incremental encoder with 11-bit resolution and incremental resolution of $5 \cdot 10^{-7}$ m. The object has been constrained to the actuator shaft through a gripper purposely realized,

which made the object travel for 0.01 m upon the test surfaces at three different velocities (0.15 m/s, 0.25 m/s, 0.35 m/s) with corresponding accelerations of 0.30 m/s^2 , 0.40 m/s^2 and 0.50 m/s^2 . In each trial, the object was fixed to the gripper so that the X-axis of the accelerometer was oriented towards the gravity direction (Fig. 5b), thus yielding the response with the greatest amplitude.

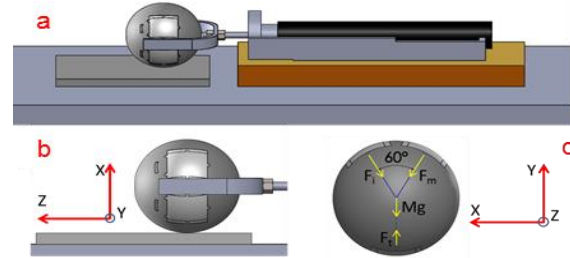


Fig. 5. Slip set-up with test surface and linear actuator (a); detail of the accelerometer axes during slip tests (b); detail of the accelerometer axes and forces scheme during the grasp trial without slip (c).

Fig. 6 shows the Power Spectrum Density (PSD) of the X-axis for the three trials performed on each surface. The significant frequency ranges tend to decrease with the roughness, ranging from 700 Hz for $32 \cdot 10^{-7}$ m roughness to below 100 Hz for $2 \cdot 10^{-7}$ m roughness, enabling slippage detection also for very low roughness values.

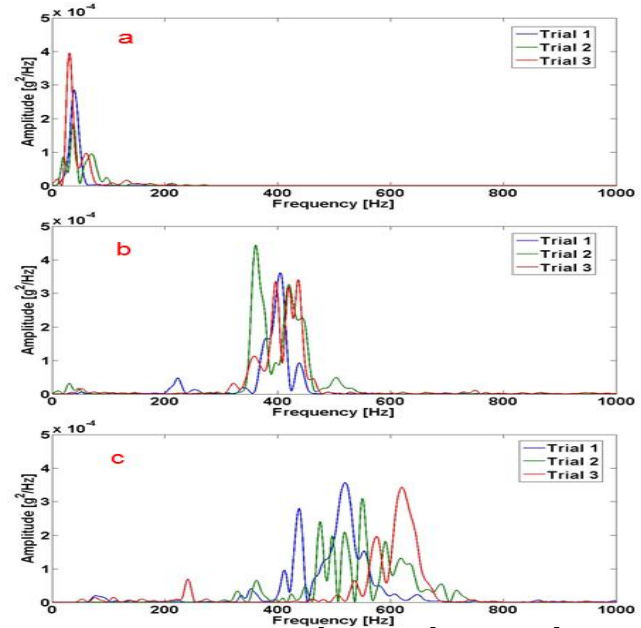


Fig. 6. PSDs for roughness: $2 \cdot 10^{-7}$ m (a), $8 \cdot 10^{-7}$ m (b), $32 \cdot 10^{-7}$ m (c).

C. Grasp analysis with human hand

One human subject was required to grasp the object and to steadily hold it, according to Fig. 5c. At the equilibrium (stable grasp) measured forces are expected to respect the following relation:

$$F_t = Mg + (F_i + F_m) \cdot \sin\left(\frac{\pi}{3}\right) \quad (3)$$

where F_t , F_i and F_m are the forces exerted by thumb, index and middle fingers, respectively, while M is the mass of the object and g is the gravity acceleration. Figure 7 depicts the force trends of one representative trial performed by the human subject. Considering the force values between the two

vertical black bars, it can be stated that they respect (3), with a mean error of 0.12 N (± 0.06).

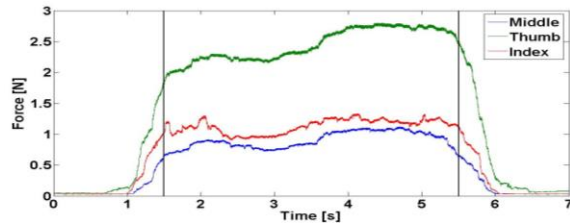


Fig. 7: forces exerted by human fingers during one representative trial.

Additionally, the subject was also required to grasp the object oriented as in Fig. 5b, and then to slightly release it until the object fell (in order to simulate slippage conditions). Figure 8 shows the outputs of both FSR sensors and accelerometer, demonstrating the ability of the latter to sense slip events. Again, for sake of clarity, only the axis directed towards gravity direction is considered (X-axis). Black bars delimitate the window (10^{-1} s) used for spectral analysis: it has been chosen immediately before the object fall, which is highlighted by the peak in the accelerometer signal. It is in this time window that incipient slip occurs, as forces critically decrease. Spectral content corresponding to the slippage event is concentrated below 100 Hz: this is reasonable, considering the very smooth surface of the object.

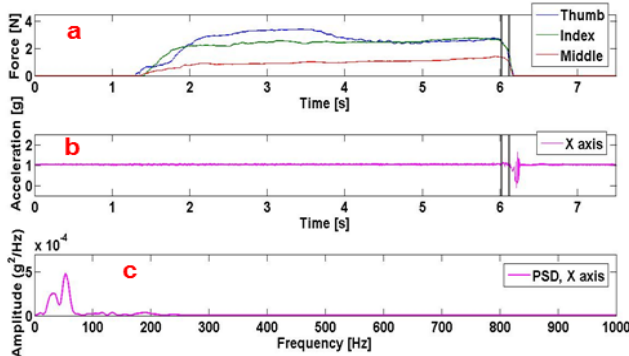


Fig. 8. Fingers forces (a), X component of acceleration (b), and corresponding PSD (c).

IV. CONCLUSIONS AND FUTURE WORKS

In this paper the development and preliminary testing of an instrumented object for evaluating the applied force during grasping have been illustrated. Results of forces behavior might be employed for improving grasping algorithms relying only on kinematic data [24]. The object embedded sensors for force and acceleration measurements and an electronic board for collecting the outputs signals from the sensors. The reliability of the instrumented object has been evaluated by: (i) comparing force sensors measures with a ground truth; (ii) investigating the accelerometer abilities to detect slippage for different roughness values; (iii) assessing grasp trials performed by a human subject with the object. The obtained results encourage to utilize the designed object as an evaluating tool for grasp capabilities in humans as well as in robotic hands. Future works will be addressed to: (i) use the accelerometer for estimating the object orientation, thus, eliding the gravity components due to object weight in different configurations; (ii) perform a

statistical analysis of the results gathered with different subjects and possibly with different robotic hands; (iii) increase the number of instrumented objects for analyzing different types of grasps.

REFERENCES

- [1] P. Saccomandi, E. Schena, C. M. Oddo, L. Zollo, S. Silvestri and E. Guglielmelli, "Microfabricated Tactile Sensors for Biomedical Applications: A Review," *Biosensors*, vol. 4, pp. 422-448, 2014.
- [2] N. Hendrich, D. Klimentjew, Z. Jianwei, "Multi-sensor based segmentation of human manipulation task", *Multisensor fusion and integration for intelligent systems*, 2010.
- [3] A. Kargov, C. Pylatiuk, S. Schulz, L. Dderlein, "A comparison of the grip force distribution in natural hands and in prosthetic hands", *Disability and Rehabilitation*, vol. 26 no. 12, pp. 705-711, 2004.
- [4] J.R. Flanagan, A.M. Wing, "Modulation of grip force with load force during point-to-point arm movements", *Experimental Brain Research*, vol. 95, no. 1, pp. 131-143, 1993.
- [5] R.S. Johansson, K.J. Cole, "Grasp stability during manipulative actions", *Can J Physiol Pharmacol*, vol. 72, pp. 511-524, 1994.
- [6] W.D. Memberg, P.E. Crago, "Instrumented objects for quantitative evaluation of hand grasp", *J Rehabil Res Dev*, vol. 34, pp. 82-90, 1997.
- [7] T. Keller, M.R. Popovic, M. Ammann, C. Anderegg, C. Dumont, "A system for measuring finger forces during grasping", *International Functional Electrical Stimulation Society Annual Conference*, 2000.
- [8] W.D. Memberg, P.E. Crago, "A grasp force and position sensor for the quantitative evaluation of neuroprosthetic hand grasp system", *IEEE Transactions on rehabilitation engineering*, vol. 3, no. 2, 1995.
- [9] R. Koiva, R. Haschke, H. Ritter, "Development of an intelligent object for grasp and manipulation research", *International Conference on Advanced Robotics*, pp. 204-210, 2011.
- [10] M.A. Roa, R. Koiva, C. Castellini, "Experimental Evaluation of Human Grasps Using a Sensorized Object", *IEEE RAS/EMBS International Conference on Biomedical Robotics and Biomechatronics*, 2012.
- [11] J.R. Flanagan, M.K.O. Burstedt, et al., "Control of fingertip forces in multidigit manipulation", *J Neurophysiol*, vol. 81, pp. 1706-1717, 1999.
- [12] G. Baud-Bovy, J.F. Soechting, "Two virtual fingers in the control of the tripod grasp", *J. Neurophysiol*, vol. 86, no. 2, pp. 604-615, 2001.
- [13] M.K.O. Burstedt, J. Randall Flanagan, R.S. Johansson, "Control of Grasp Stability in Humans Under Different Frictional Conditions During Multidigit Manipulation", *The American Physiological Society*, 1999.
- [14] A. Serio, E. Riccomini, V. Tartaglia, I. Sarakoglou, M. Gabiccini, N. Tsagarakis, A. Bicchi, "The Patched Intrinsic Tactile Object: a Tool to Investigate Human Grasps", *IEEE/RSJ International Conference on Intelligent Robots and Systems*, 2014.
- [15] R.D. Howe, M.R. Cutkosky, "Sensing skin acceleration for slip and texture perception", *IEEE International Conference on Robotics and Automation*, vol. 1, pp. 145-150, 1989.
- [16] M.R. Tremblay, W. J. Packard, M.R. Cutkosky, "Utilizing Sensed Incipient Slip Signals for Grasp Force Control", *Japan-USA Symposium on Flexible Automation*, 1992.
- [17] M.R. Tremblay, M.R. Cutkosky, "Estimating Friction Using Incipient Slip Sensing During a Manipulation Task", *IEEE International Conference on Robotics and Automation*, vol. 1, pp. 429-434, 1993.
- [18] L.E. Rodriguez-Cheu, A. Casals, "Sensing and control of a prosthetic hand with myoelectric feedback", *IEEE BioRob*, pp. 607-612, 2006.
- [19] V. Abhinav, S. Vivekanandan, "Real-Time Intelligent Gripping System for Dexterous Manipulation of Industrial Robots", *World Congress on Engineering*, vol. 2, 2009.
- [20] A. Cloutier, J. Yang, "Design, Control, and Sensory Feedback of Externally Powered Hand Prostheses: A Literature Review", *Critical Reviews in Biomedical Engineering*, vol. 41, no. 2, pp. 161-181, 2013.
- [21] R.S. Figliola, D.E. Beasley, "Basic concepts of measurement methods, in Theory and Design for Mechanical Measurement", *John Wiley & Sons*, 5th ed., p. 20, 2010.
- [22] http://www.interlinkelectronics.com/datasheets/Datasheet_FSR.pdf
- [23] H. Liu, K. Wu, P. Meusel, N. Seitz, G. Hirzinger, M.H. Jin, Y.W. Liu, S.W. Fan, T. Lan, Z.P. Chen, "Multisensory Five-Finger Dexterous Hand: The DLR/HIT Hand II", *IEEE/RSJ IROS*, pp. 3692-3697, 2008.
- [24] F. Cordella, L. Zollo, A. Salerno, D. Accoto, E. Guglielmelli, B. Siciliano, "Human Hand Motion Analysis and Synthesis of Optimal Power Grasps for a Robotic Hand", *IJARS*, vol. 11, no. 37, pp. 1-13, 2014.